ELSEVIER

Ceramics International 30 (2004) 2295–2303

CERAMICS INTERNATIONAL

www.elsevier.com/locate/ceramint

Morphology and sintering behaviour of yttria stabilised zirconia (8-YSZ) powders synthesised by spray pyrolysis

Manuel Gaudon [a], Elisabeth Djurado [b], Norbert H. Menzler [c,*]

[a] *CIRIMAT/LCMIE, Université Paul Sabatier, Bat IIR1, 118 Route de Narbonne, 31062 Toulouse Cedex 4, France*
[b] *Laboratoire d'Electrochimie et de Physico-Chimie des Matériaux et des Interfaces LEPMI, 1130 Rue de la Piscine, 38402 St. Martin d'Heres Cedex, France*
[c] *Forchungszentrum Jülich GmbH, Institute for Materials and Processes in Energy Systems, IWV-1, 52425 Jülich, Germany*

Received 16 October 2003; received in revised form 21 November 2003; accepted 5 January 2004
Available online 21 April 2004

Abstract

This work is focused on the synthesis of nano-crystallised yttria stabilised zirconia (YSZ) powders by the spray pyrolysis method, the aim of the study being a better understanding of the influence of the spray pyrolysis parameters on the morphology of the produced powders. Spray pyrolysed powder consists of polycrystalline particles, which are spherical. Each particle consists of nanometric primary grains. The morphology of these polycrystalline particles was characterised by scanning electron microscopy (SEM), helium pycnometry, thermogravimetric analysis (TGA) and mass spectroscopy (MS), and the results are compared. Thus, particle size, particle size distribution and particle porosity were determined and correlated to the process parameters. Finally, by dilatometric measurements, sintering curves of pellets prepared from different sets of powders were analysed in regard of their morphologies. Two main conclusions could be deduced from these studies. Firstly, the process parameters influence both internal porosity and particle size distribution of the synthesised powders. Secondly, the morphologies of the spray pyrolysed nano-powders lead to particularly high sintering activities.

Keywords: A. Sintering; Spray pyrolysis; Yttria stabilised zirconia; Submicron powders

1. Introduction

Homogeneous metal oxide powders used in many technical applications should have submicron size, uniform morphology and high purity. Yttria stabilised zirconia (YSZ) is usually used as electrolyte material for solid oxide fuel cells (SOFCs). At the present time, the performance of electrolyte-supported SOFC is mainly limited by the ohmic loss through the thick electrolyte. It is why many recent investigations deal with the reduction of the electrolyte thickness of 5–10 μm [1–5]. The most useful and lowest cost routes for preparing a dense layer of YSZ are based on wet chemical coating processes, such as screen printing [6,7], vacuum slip casting and slip casting [8–10], tape casting [11–13], wet powder spraying [14–16] and sol–gel processes [17]. To obtain a very thin layer, the key point in all these processes is to use a submicron starting powder, taking care that powder particles are fully dispersed in the suspension.

Spray pyrolysis is a production route which allows the synthesis of complex oxides at low temperatures and thus leads to submicron powders; it therefore can be described as a soft chemistry process. Spray pyrolysis is a process well suited to the production of YSZ submicron powders [18–22]. In a particular example [23], with aqueous starting solution of zirconyl nitrates and yttrium nitrates, the process easily leads to the production of tetragonal or cubic yttria stabilised zirconia at 600 °C, i.e. just after the nitrate groups decomposition. Furthermore, with this process the powders are calcined in a very short time: 1–10 s. Then, the oxides produced by the spray pyrolysis process are composed of polycrystalline particles with submicron size which consist of nano-sized primary grains. The control of the primary particle diameter using the process parameters is one of the most important advantages of this synthesis method. Submicron spherical particles can be easily obtained. In addition, while all spherical aerosol droplets are separately pyrolysed in a

* Corresponding author. Fax: +49-2461-612455.
E-mail address: n.h.menzler@fz-juelich.de (N.H. Menzler).

0272-8842/$30.00 © 2004 Elsevier Ltd and Techna S.r.l. All rights reserved.
doi:10.1016/j.ceramint.2004.01.010

short time to form discrete solid particles, a good dispersion of these powders in any solvent is very easy to achieve in comparison to powders from other methods such as sol–gel or co-precipitation.

In the first part of this paper an investigation of the influence of the process parameters on the mean diameter and particles size distribution of cubic YSZ powders with composition ZrO_2–8 mol% Y_2O_3 (8-YSZ) is reported. In the second part, the sintering behaviour of different spray pyrolysed powders is examined and correlated to their morphologies and preparation parameters.

2. Experimental

2.1. Powder preparation

The 8-YSZ zirconia powders were prepared by the spray pyrolysis technique using an ultrasonic atomiser. The precursor solutions were prepared from a stoichiometric mixture of zirconyl nitrate hydrate $ZrO(NO_3)_2{\cdot}6H_2O$ and yttrium nitrate hydrate $Y(NO_3)_3{\cdot}6H_2O$ dissolved in distilled water. The concentration investigated was fixed to 2.5×10^{-2} mol l^{-1}. These solutions were atomised by a high-frequency ultrasonic mist generator. In this study, two piezoelectric ceramic transducers were used for which the frequencies were 2.5 and 1.7 MHz. Here, it is worth to note that the atomisers contained three ceramic transducers. The produced aerosol was carried through a tubular furnace with air (N_2–O_2 mixture) flow rate of 6 l min^{-1}. The temperature of the tubular furnace was fixed at 600 or 1100 °C.

2.2. Powder characterisation

The crystallographic structures of the sprayed powders were characterised by X-ray diffraction using a Siemens D-500 diffractometer. The achievement of a pure YSZ cubic phase after the spray pyrolysis procedure was checked in all cases, and the grain sizes of the powders were evaluated from XRD patterns applying the Scherrer formula. The thermal decomposition of the oxide particles obtained by the spray pyrolysis process was studied by two techniques. Firstly, thermogravimetric analysis (TGA) using a Setaram 92B thermobalance (accuracy 10^{-4} g) with a heating rate of 3 °C min^{-1} was used. The second technique was gaseous effluent analysis during the decomposition steps using a Balzers QMG 421 mass spectrometer.

The particle morphologies were examined using a scanning electron microscope (Jeol JSM 6400). The particle size distribution was evaluated from image treatment of the scanning electron micrographs (using Image.tool software). The particle density was measured with a double room helium pycnometer (Micromeritics-AccuPyc 1330). Calculations were then carried out using the ideal gas law (accuracy on particle density was estimated at about 1%). Finally, the sintering behaviour of green pellets, 8 mm in diameter, obtained from uniaxial pressure ($P = 300$ MPa) of the sprayed powders was studied by dilatometric analyses. The dilatometric experiments and more particularly the sintering curves have been recorded using a push-rod dilatometer (Netzsch 402 E). Sintering of the pellets was performed at 1400 °C for 5 h with a heating rate of 3 °C min^{-1} (same conditions than for TGA analyses).

3. Results and discussion

Previous investigations of spray pyrolysis process [23–25] were performed to prepare undoped zirconia and low Y_2O_3-doped nano-powders of tetragonal polycrystalline zirconia. In this work, the influence of synthesis parameters on the transformation step from aerosol droplets to solid particles was investigated. Furthermore, in the literature, many studies dealing with this subject were found [26–28]. From all these studies, it can be concluded that four parameters have to be taken in consideration: the atomising frequency of the piezoelectric ceramics, the concentration of metallic salts in the starting solution, the flow rate of the aerosol in the tubular furnace, and the furnace temperature. The mentioned parameters can be divided in two groups: (i) the atomising frequency is the key parameter for control of the droplet size of the aerosol (in this first group), the density of the precursor solution and its surface tension have an influence too, but here, these parameters will be considered the same in both sets; (ii) the concentration, the carrier gas flow rate and the furnace temperature influence the transformation of the liquid droplets into final oxide particles, i.e. on the oxide particles morphology (size, density, etc.). Here, two parameters have been studied with great attention: the atomising frequency and the furnace temperature.

3.1. Influence of atomising frequency

To study only the influence of atomising frequency, the other three parameters had to be fixed. It can be recalled that based on previous work [23] the metallic salts concentration in the aqueous starting solution is fixed at 2.5×10^{-2} M and the gas flow rate is fixed at 6 l min^{-1}. Furthermore, for this study, a furnace temperature of 600 °C was chosen. Thus, two series of 8-YSZ powders from the two atomising frequencies (1.7 and 2.5 MHz) were produced and the two resulting oxide powders will be referred as YSZ-1.7-600 and YSZ-2.5-600 in the following.

The forced oscillating frequency of the ultrasonic atomiser creates equivalent oscillations of the liquid column in the sprayer dish, causing development of transverse longitudinal disturbances. Their superposition depends on the surface tension, liquid viscosity, liquid column height, the number of the piezoelectric ceramics used to produce the oscillating frequency, dish shape and position of piezoelectric ceramics in the dish, and more particularly forced frequencies of the oscillators. Assuming that waves of spherical diameter are

created and boundary conditions where the liquid velocity at the sides of the dish is equal to zero, the mean diameter of the aerosol droplets can be determined using Lang's equation [29]

$$D = 0.34 \times 10^6 \left(\frac{8\pi\sigma}{\rho f^2}\right)^{1/3} \quad (1)$$

where D is the aerosol droplet diameter (μm), σ is the surface tension of the precursor solution ($N\,m^{-1}$), r is the solution density ($g\,cm^{-3}$), and f is the frequency of the piezoelectric ceramic oscillator (Hz). Considering that the nitrate salts have no influence on σ and ρ, for frequencies of 1.7 and 2.5 MHz, expected mean droplets sizes are 2.70 and 2.08 μm, respectively.

From SEM micrographs of solid oxide particles obtained at the end of the process, the influence of the atomising frequency on aerosol droplets diameter can be derived using the following equations linking aerosol droplet diameter with theoretical and experimental oxide particle diameters

$$d_0 = 10^3 \left(10^{-3} \times \frac{CMD^3}{\rho_{ox}}\right)^{1/3} \quad (2)$$

$$p = 100 \left(\frac{d_{exp}^3 - d_0^3}{d_{exp}^3}\right) \quad (3)$$

where d_{exp} is experimental mean diameter of the oxide particles (nm), d_0 is theoretical mean diameter of the oxide particles (nm) (considering that all the particles are dense), C is the equivalent concentration of YSZ oxide in the starting nitrate solution in ($mol\,l^{-1}$), M is the molar mass of YSZ ($g\,mol^{-1}$), ρ_{ox} is theoretical YSZ oxide density ($g\,cm^{-3}$), and p is the porosity percentage of the experimental spherical particles. The theoretical diameter d_0 expected from the Lang's equation for frequencies of 1.7 or 2.5 MHz are 216 and 166 nm, respectively.

SEM micrographs of YSZ-2.5-600 and YSZ-1.7-600 powders are shown in Fig. 1 and Fig. 2a, respectively. The particle size distribution obtained by image treatment of SEM micrographs relative to both powders are shown in Figs. 3 and 4, respectively. On SEM micrographs, it can be seen that the obtained particles are perfectly spherical with smooth surfaces. Several aspects concerning the particle size distribution have to be discussed.

Firstly, the powders are more or less widely and multimodally distributed according to the frequency used. Jokanovic and coworkers [30,31] have demonstrated that powders from spray pyrolysis have a distribution spectrum of a series of values corresponding to a set of resonant liquid column frequencies for different factors of wave shapes, dependent on different damping factors of transverse and longitudinal waves generated by ultrasonic excitation. In our case, the particle size distribution was wider when the frequency used was 2.5 MHz than for 1.7 MHz (please note the different scales of the x-axes in Figs. 3–5). From Jokanovic et al., it appears that the process of harmonisation of the forced field of the two ultrasonic generators with the field of frequencies characteristic of the system are very different between these two experiments. One may conclude that the spray pyrolysis process is very promising for achieving powders synthesised with very different particle size distribution (wide or narrow distribution). To conclude, particle size and particle size distribution are fully dependant on the frequency of the ultrasonic atomiser in the pyrosol process.

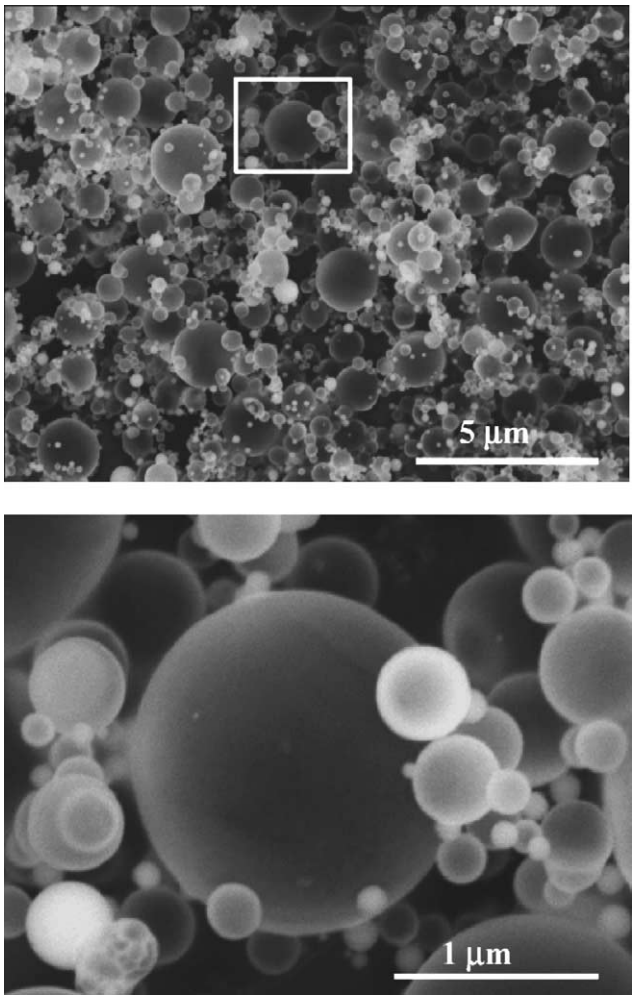

Fig. 1. SEM micrographs of solid particles obtained at 600 °C with an atomising frequency of 2.5 MHz.

Secondly, assuming the mean experimental diameters d_{exp} of both distribution spectra corresponding to the centre of the distribution, i.e. diameters d_{exp} corresponding to the larger particles population, they can be compared with the value predicted by Lang's equation. As shown in Figs. 3 and 4, the mean experimental diameters for 1.7 and 2.5 MHz are 235 and 180 nm, respectively. In both cases, the experimental diameters (d_{exp}) are about 10% higher than the theoretical ones predicted by Lang's equation (d_0). The hypothesis that the obtained particles exhibit a closed porosity seems to be valid to justify d_{exp} and d_0 differences. Applying Eq. (3) in both cases (for 1.7 and 2.5 MHz) the calculated porosity is

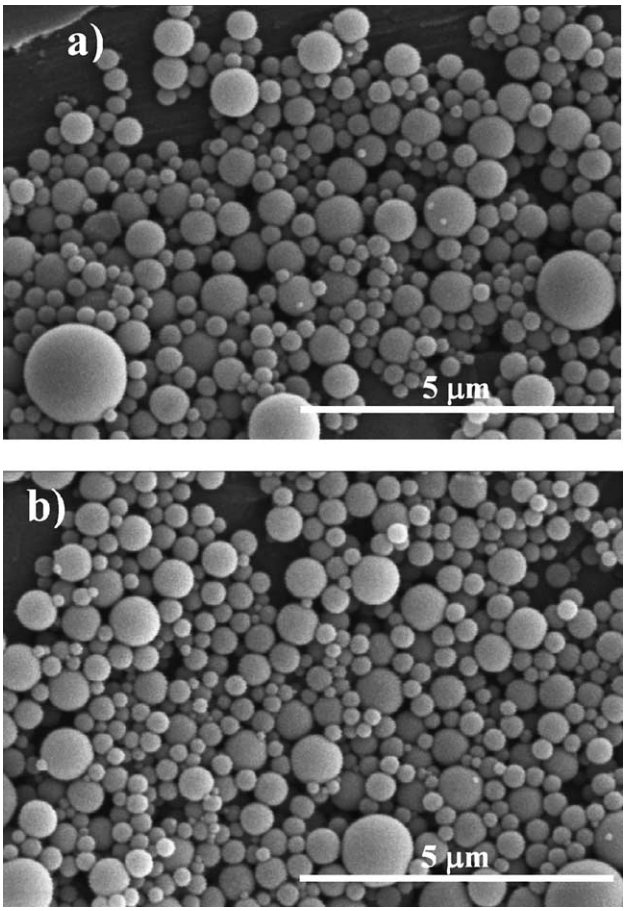

Fig. 2. SEM micrographs of solid particles obtained with an atomising frequency of 1.7 MHz with a tubular furnace temperature of (a) 600 °C and (b) 1100 °C.

found close to 20 vol.%. To verify this last hypothesis, the influence of the furnace temperature has been studied.

3.2. Influence of furnace temperature

The flow rate and the furnace temperature are known to be the most influential parameter on the final solid particles. These two parameters are linked but in practice, differences exist between authors on the real influence of these parameters. As Messing et al. [32] have shown, the evaporation stage of the process can be described as a series of physical phenomena occurring simultaneously. Thus, it is very difficult to predict the influence of the parameters on the density of sprayed particles. To obtain a good yield (describing here the ratio between production in g and time in h), flow rate has to be sufficient. In [23], four different morphologies of undoped zirconia final powders were reported as smooth or grained, distorted or multi-layered spheres as function of pyrosol conditions. The flow rate was fixed here at 6 l min^{-1} and calcination temperatures were 600 and 1100 °C. In order to study the influence of the furnace temperature on the morphology of YSZ particles, the atomising frequency was fixed at 1.7 MHz. The two series of subsequently synthesised powders are designated YSZ-1.7-600 and YSZ-1.7-1100, hereafter.

Firstly, XRD measurements confirmed that a pure cubic phase was obtained for each calcination temperature; the grain sizes evaluated with the Scherrer formula were found to be around 5–6 nm for the furnace temperature of 600 °C and 15–20 nm at 1100 °C. In both cases, even for a calcination temperature of 1100 °C, because of the velocity of the process, nano-sized grains materials were obtained. Secondly, helium pycnometry measurements were performed on the two series of powders: the densities were 4.708 and 5.780 g cm^{-3} for 600 and 1100 °C, respectively. Taking into

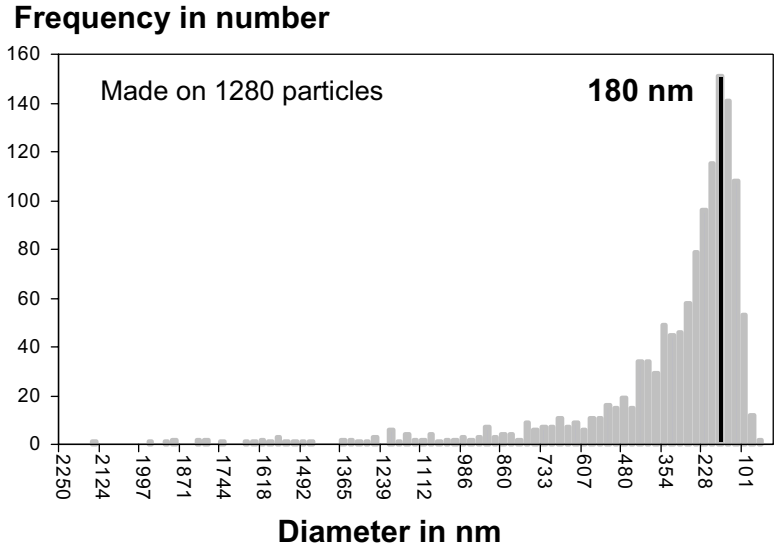

Fig. 3. YSZ-2.5-600 particle size distribution obtained by image treatment of SEM micrographs.

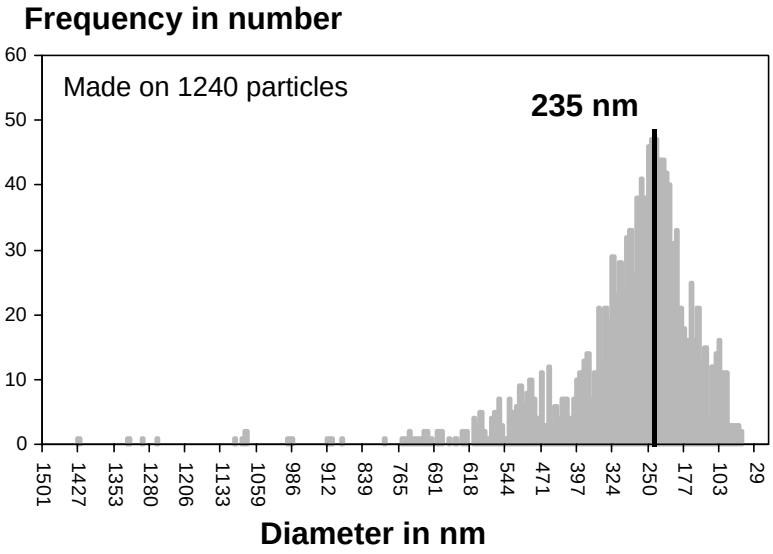

Fig. 4. YSZ-1.7-600 particle size distribution obtained by image treatment of SEM micrographs.

account a theoretical density of 5.96 g cm^{-3} for 8-YSZ oxide, densities of the YSZ-1.7-600 and YSZ-1.7-1100 are found about 80 and 97%, respectively. The density of 80% of the powder calcined at 600 °C maybe not quite correct due to the fact that the temperature of 600 °C is not sufficient to burn out or decompose all nitrate phases. Thus, the theoretical density must be assumed as a sum of the density of pure 8-YSZ and the density of the remaining nitrates. These results confirm that the porosity of sprayed powders can be controlled by means of the tubular furnace temperature; here, an increase of the calcination temperature induced a large increase in the particle density. Therefore, to understand the cause of the internal porosity in the YSZ-1.7-600 powder, TGA coupled with mass spectroscopy were performed on this powder. The results are presented in Figs. 6 and 7. It can be seen (Fig. 6) that two main mass losses were detected by TGA: the first one occurred between 60 and 150 °C; the second one occurred between 450 and 750 °C. The first loss can be qualitatively attributed to water evaporation and the second one to nitrate decomposition as detected by mass spectroscopy (Fig. 7). Quantitative studies on nitrate proportions are very difficult, but this experiment shows that the decomposition of the nitrates is not complete at 600 °C, the selected temperature of the pyrosol furnace. Consequently, the YSZ-1.7-600 powder particles remain porous after spray pyrolysis synthesis.

The influence of the furnace temperature on particle distribution of this second set of powder was, in a final study, investigated using SEM analyses performed with image treatment. A SEM micrograph is shown in Fig. 2b and the

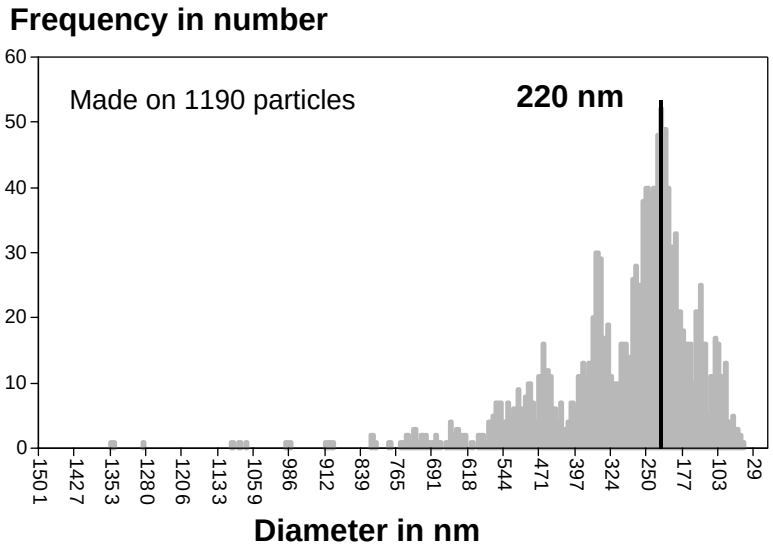

Fig. 5. YSZ-1.7-1100 particle size distribution obtained by image treatment of SEM micrographs.

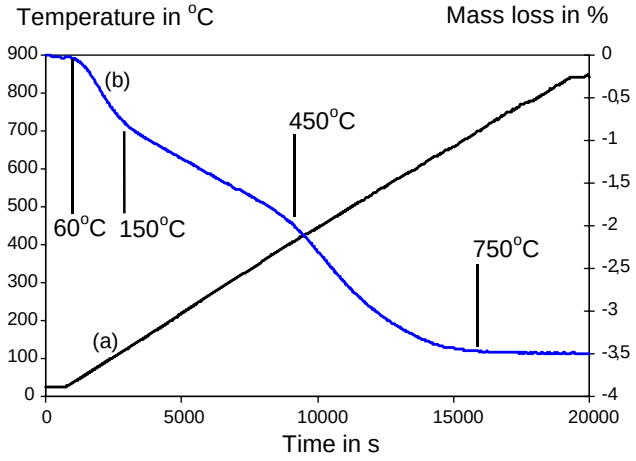

Fig. 6. Thermogravimetric analyses of YSZ-1.7-600 powder. (a) Temperature curve; (b) mass loss (in %).

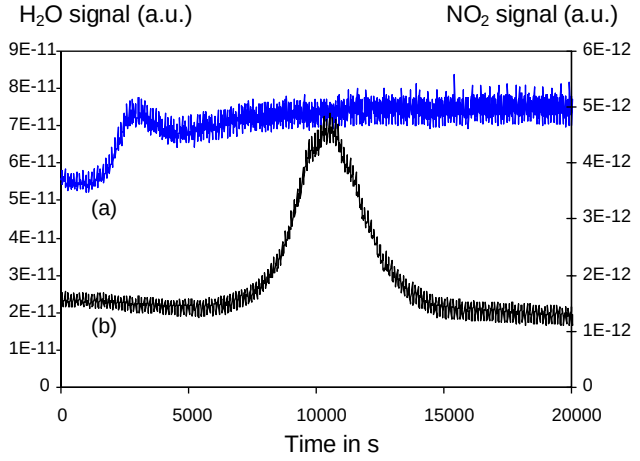

Fig. 7. SM effluents signal of YSZ-1.7-600 powder. (a) H_2O signal; (b) NO_2 signal.

corresponding particle size distribution is in Fig. 5. At first sight, no differences can be seen between the two SEM micrographs of Fig. 2a and b. However, it can be seen that the corresponding size distribution from image treatment is slightly different. In comparison with YSZ-1.7-600 sample, the YSZ-1.7-1100 distribution spectrum is better defined. Indeed, the secondary maxima of the distribution spectrum can be clearly observed here (e.g. at about 350 and 460 nm). It can be deduced that the YSZ-1.7-1100 spectrum is sharper than the YSZ-1.7-600 spectrum because in the first case both prepared particles must be dense, and in the second case, a variation of porosity content from one particle to another one may affect the spectrum by smoothing the distribution profile.

Besides some of the aimed applications for these powders (production of dense layers for SOFC electrolytes or porous layers for thermal barrier coatings), the consequences of the absence or presence of internal porosity in the powder particles for their sintering behaviour can be important and have to be investigated. Such study is presented in the last part of this paper.

3.3. Sintering behaviour

The sintering curves on the YSZ-1.7-600, YSZ-2.5-600 and YSZ-1.7-1100 pellets are presented in Fig. 8.

The sintering curves of YSZ-1.7-600 (Fig. 8a) and YSZ-2.5-600 (Fig. 8b) were compared. The characteristics of both sintering curves are very similar, and can be divided into three steps. A first shrinkage occurs between 450 and 780 °C. This first step can be correlated with the nitrate decomposition step detected by TGA measurements. At this stage of the work, it can be already assumed that this step occurring at very low temperatures is linked to the internal porosity of the particles between each primary grain. A second step occurs between 780 and 1150 °C, and then, a third one occurs over 1150 °C. Even if the sintering curves present

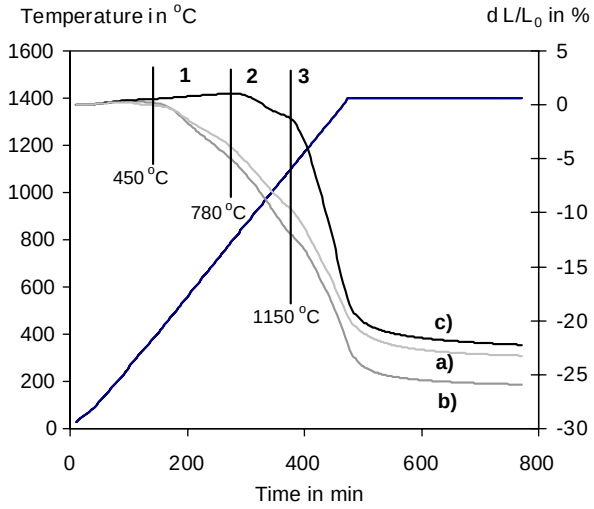

Fig. 8. Sintering curves of pellets made from spray pyrolysed powder: (a) YSZ-1.7-600 set, (b) YSZ-2.5-600 set, (c) YSZ-1.7-1100 set.

the same evolution for these two samples, the total shrinkage at the end of the sintering process is different. Indeed, the YSZ-2.5-600 sample exhibited a shrinkage of around 10% more than the YSZ-1.7-600 sample. Pellet green density and pellet final density are summarised in Table 1. The densities were calculated from the mass and volume measurements. The difference in shrinkage and so, final density, between the two samples: 96% for YSZ-2.5-600 and 89.5% for YSZ-1.7-600, cannot be explained only by a small difference

Table 1
Density of green and sintered pellets made from the different samples (calculations are based on mass to volume ratio)

Samples	Pellets green density (%)	Pellets final density (%)
YSZ-1.7-600	54.5	89.5
YSZ-2.5-600	56.5	96
YSZ-1.7-1100	67	97

in their green densities. Both calculated final densities can be compared to the SEM micrographs presented in Fig. 9. Since both samples present exactly the same sintering curve steps, an explanation based on different mechanisms of sintering is not possible. From previous experiments, it appears obvious that the explanation of such observations can be correlated with the particle size distribution. Indeed, the particle size distribution of the YSZ-2.5-600 sample was wider than that of the YSZ-1.7-600 sample. Background knowledge shows that for many ceramic processes, for example slip casting or tape casting processes, a wide grain size distribution of particles leads to easier sintering ceramic (one can refer to the Bernache-Assolant's book [33]). In our case, i.e. with perfectly spherical particles and multimodal size distribution, differences in the final density seems to be amplified.

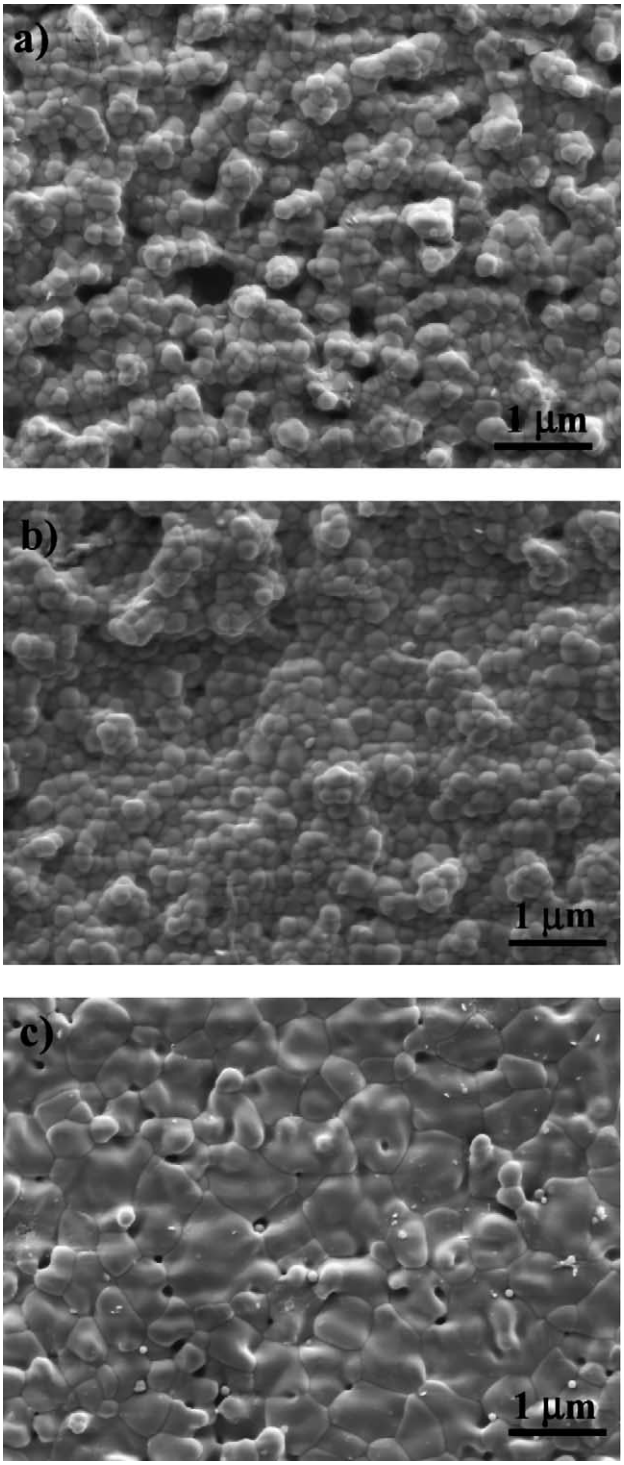

Fig. 9. SEM micrographs of sintered pellets made from spray pyrolysed powder: (a) YSZ-1.7-600 set, (b) YSZ-2.5-600 set, (c) YSZ-1.7-1100 set.

The last point to discuss from the comparison of these two first samples is the grain size of the final ceramic, which can be easily calculated from the two micrographs (Fig. 9). It can be seen on the two micrographs corresponding to these two samples (YSZ-1.7-600 and YSZ-2.5-600) that pellets had different porosities but nearly the same grain sizes. The average particle size for both samples was very low, about 50–200 nm. It seems that the particle shape and diameter of the particles remained practically unchanged during sintering. This is consistent with previous work on tetragonal polycrystalline zirconia ceramics [34]. It could be explained by the presence of inter-particle porosity from one point but also because of high purity of the materials.

Secondly, in order to study the influence of the tubular furnace temperature on the sintering curves, the final density and the final grain sizes of YSZ-1.7-1100 have to be compared to the preceding curves. Here, the most important phenomenon point is that the first shrinkage step did not occur for the YSZ-1.7-1100 because the raw powder was prepared precisely at 1100 °C. However, because the starting powder particles were dense in this case, the green density obtained for this sample was larger than for the two previous ones (see Table 1). Furthermore, the final grain size reached after sintering was significantly more important than in the two previous cases (nearly 1 μm, see Fig. 9). This phenomenon seems to be the consequence of the more pronounced third sintering step. It proves that the internal porosity inside the particles of the two previous samples was the reason of the limitation of the grain size growth during sintering. For this last pellet, the absence of closed porosity inside the pre-sintered primary particles allowed a higher degree of sintering at 1400 °C than in the previous cases. Thus, a good final density was reached for this last sample (97%).

From both sintering behaviour studies, it was proved that the first shrinkage step occurring at very low temperatures in the two first samples corresponds to a partial disappearance of the particle internal porosity. The very small sizes of these inclusion pores located inside the primary particles as well as the presence of nano-grains may explain the very low temperature of the first shrinkage step (450–750 °C). Furthermore, these inclusion pores seem to explain the very small grain sizes reached after sintering (50–200 nm at 1400 °C). The two last sintering steps occurring in all three samples probably corresponds to the suppression of inter-particle porosity and inter-agglomerate

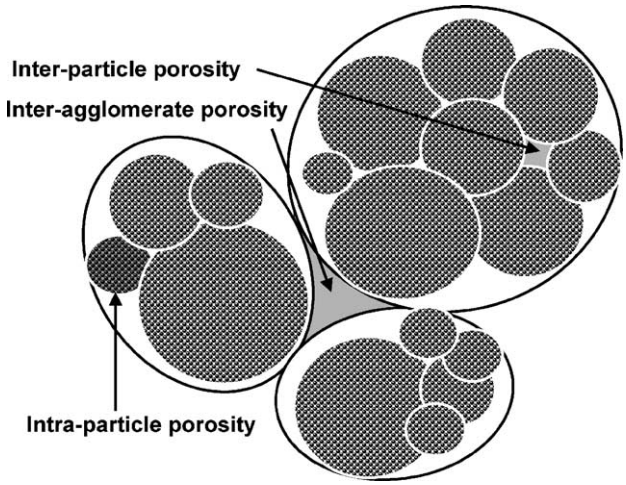

Fig. 10. Schematic representation of a microscopic area of the YSZ-1.7-600 green pellet.

porosity, respectively. Indeed, because the pellets are made of submicron primary particles, it seems to be difficult to avoid the appearance of agglomerates.

A schematic representation of the different kinds of pore located in a characteristic green pellet of sprayed powder is shown in Fig. 10 and can be related to the main conclusions presented in this discussion.

4. Conclusions

The main goal of this paper was a better understanding of the influence of the two main parameters of the spray pyrolysis process on the YSZ particle morphologies (particle size, particle size distribution and porosity) and on their sinterability.

Firstly, it could be shown that particle size distribution could be described by a distribution spectrum, as already proposed by Jokanovic et al. The atomising frequency and the shape of the ultrasonic generator could have led to dramatic changes in the width of this spectrum. Furthermore, with perfectly spherical particles as produced by spray pyrolysis, the influence of the distribution spectrum width on the sinterability of these powders was very important. Beside applications, it has been shown that a wide particle size distribution is preferable for providing dense ceramics. However, the multitude of process parameters and their interactions make it difficult to obtain a perfect control of the final distribution spectrum.

Secondly, it has been proved that primary particles produced by the spray pyrolysis can result in the internal porosity varying in a large range (from about 3 to 20%) according to the calcination temperature of the aerosol droplets during the process. Besides sintering application, of course, the synthesis of dense particles led to ceramics which were easier to densify at relatively low temperatures. The higher the spray pyrolysis temperature, the denser the particles (the larger the densification). However, from a fundamental point of view, it has been shown that, due to internal porosity, sintering occurred in a very low temperature range, never before observed for YSZ (500–800 °C). Furthermore, this internal porosity inside the starting oxide particles seemed to limit the grain growth during sintering, producing—after a sintering step at 1400 °C during 5 h—materials with grain sizes of only 50–200 nm. In consequence, spray pyrolysis appears to be an interesting new process for the production of nano-powders that remain in the submicron range even after exposure at very high temperatures.

Acknowledgements

The authors are grateful to A. Lemmens and D. Sebold for experimental assistance on dilatometric and SEM analyses. M. Gaudon thanks Prof. Stoever (IWV-1 director) for hospitality at the institute and the ability to complete the work begun at LEPMI.

References

[1] C. Barnay, M. Marchand, M. Cassir, Prospects of different fuel cell technologies for vehicle applications, J. Power Sour. 108 (2002) 139.
[2] H.Z. Song, H.B. Wang, S.W. Zha, D.K. Peng, G.Y. Meng, Aerosol-assisted MOCVD growth of Gd_2O_3-doped CeO_2 thin SOFC electrolyte film on anode substrate, Solid State Ionics 156 (2003) 249.
[3] U.G. Bossel, Solid oxide fuel cells for transportation, in: P. Stevens (Ed.), Proceedings of the Third European SOFC Forum, Lucerne, Switzerland, 1998, p. 55.
[4] W.A. Meulenberg, N.H. Menzler, H.P. Buchkremer, D. Stover, Manufacturing routes and state-of-the-art of the planar Jülich anode-supported concept for solid oxide fuel cells, Ceram. Trans. 127 (2002) 99.
[5] J. Pena, A. Martinez, F. Conde, J.M. Gonzalez-Callet, M. Vallet-Regi, In situ growth of $SrTiO_3$ thin films prepared by AACVD from strontium and titanium oxide bisdipivaloylmethanates, Solid State Ionics 101–103 (1997) 183.
[6] G.M. Christie, P. Nammensma, J.P.P. Huijsmans, Status of anode-supported–thin-electrolyte ceramic SOFC component development at ECN, in: A.J. McEvoy (Ed.), Proceedings of the Fourth European SOFC Forum, Lucerne, Switzerland, 2000, p. 3.
[7] G.Y. Kim, S.W. Eom, S.I. Moon, Cell properties of SOFC prepared by doctor blade and screen printing method, in: U. Stimming, S.C. Singhal, H. Tagawa, W. Lehnert (Eds.), Proceedings of the Fifth International Symposium on SOFC, Pennington, NJ, 1997, p. 700.
[8] C. Wang, W.L. Worrell, S. Park, J.M. Vohs, R.J. Gorte, Fabrication and performance of thin-film YSZ solid oxide fuel cells between 600 and 800 °C, in: S.C. Singhal, M. Dokiya (Eds.), Proceedings of the Sixth International Symposium on SOFC, Honolulu, USA, 1999, p. 851.
[9] D. Ghosh, G. Wang, R. Brule, E. Tang, P. Huang, Performance of anode-supported planar SOFC cells, in: S.C. Singhal, M. Dokiya (Eds.), Proceedings of the Sixth International Symposium on SOFC, Honolulu, USA, 1999, p. 822.
[10] P. Batfalsky, H.P. Buchkremer, D. Froning, F. Meschke, H. Nabielek, R.W. Steinbrech, F. Tietz, Operation and analysis of planar SOFC stacks, in: Proceedings of the Third International Fuel Cell Conference, Nagoya, Japan, 1999, p. 349.

[11] S. Majundar, T. Claar, B. Flaudermeyer, Stress and fracture behavior of monolithic fuel cell tapes, J. Am. Ceram. Soc. 68 (1986) 628.
[12] A.C. Muller, D. Herbstritt, E. Ivers-Tiffee, Development of a multilayer anode for solid oxide fuel cells, Solid State Ionics 152/153 (2002) 537.
[13] J. Van Herle, R. Ihringer, R. Vasquez Cavieres, L. Constantin, O. Bucheli, Anode supported solid oxide fuel cells with screen-printed cathodes, J. Eur. Ceram. Soc. 21 (2001) 1855.
[14] H.P. Buchkremer, U. Diekmann, L.G.J. De Haart, H. Kabs, U. Stimming, D. Stoever, Advances in the anode supported planar SOFC technology, in: U. Stimming, S.C. Singhal, H. Tagawa, W. Lehnert (Eds.), Proceedings of the Fifth International Symposium on SOFC, Pennington, NJ, 1997, p. 160.
[15] R. Wilhenhoener, W. Mallener, H.P. Buchkremer, T. Hauber, U. Stimming, Cathode processing by wet powder spraying, in: B. Thorstensen (Ed.), Proceedings of the Second European SOFC Forum, Oberrohrdorf, Switzerland, vol. 1, 1996, p. 279.
[16] J. Joergensen, P.H. Larsen, S. Primdahl, C. Bagger, Fabrication of thin anode-supported SOFCs, in: A.J. McEvoy (Ed.), Proceedings of the Fourth European SOFC Forum, Oberrohrdorf, Switzerland, 2000, p. 203.
[17] C. Sakurai, T. Fukui, M. Okuyama, Preparation of zirconia coatings by hydrolysis of zirconium alkoxide with hydrogen peroxide, J. Am. Ceram. Soc. 76 (1993) 1061.
[18] H. Ishizawa, O. Sakurai, N. Mizutani, M. Kato, Homogeneous Y_2O_3-stabilized ZrO_2 powder by spray pyrolysis method, Am. Ceram. Soc. Bull. 65 (10) (1986) 1399.
[19] H.E. Esparza-Ponce, A. Reyes-Rojas, W. Antunez-Flores, M. Miki-Yoshida, Synthesis and characterization of spherical calcia stabilized zirconia nano-powders obtained by spray pyrolysis, Mater. Sci. Eng. A343 (2003) 82.
[20] K. Okada, A. Tanka, S. Hayashi, N. Otsuka, Preparation of Al_2O_3 powders from various aluminium salts by the spray pyrolysis method, J. Mater. Sci. Lett. 12 (1993) 854.
[21] F.L. Yuan, C.H. Chen, E.M. Kelder, J. Schoonman, Preparation of zirconia and yttria-stabilized zirconia (YSZ) fine powders by flame-assisted ultrasonic spray pyrolysis (FAUSP), Solid State Ionics 109 (1998) 119.
[22] N.H. Menzler, D. Lavergnat, F. Tietz, E. Sominski, E. Djurado, G. Pang, A. Gedanken, H.P. Buchkremer, Materials synthesis and characterization of 8YSZ nanomaterials for the fabrication of electrolyte membranes in solid oxide fuel cells, Ceram. Int. 29 (2003) 619.
[23] E. Djurado, E. Meunier, Synthesis of doped and undoped nanopowders of tetragonal polycrystalline zirconia (TPZ) by spray-pyrolysis, J. Solid State Chem. 141 (1998) 191.
[24] F. Boulc'h, M.-C. Schouler, P. Donnadieu, J.M. Chaix, E. Djurado, Domain size distribution of Y-TZP nano-particles using XRD and HRTEM, Image Anal. Stereol. 20 (2001) 157.
[25] E. Djurado, L. Dessemond, C. Roux, Phase stability of nanostructured tetragonal zirconia polycrystals versus temperature and water vapor, Solid State Ionics 136/137 (2000) 1249.
[26] J.M. Nedeljkovic, Z.V. Saponjic, Z. Rakocevic, V. Jokanovic, D.P. Uskokovic, Ultrasonic spray pyrolysis of TiO_2 nanoparticles, Nanostruct. Mater. 9 (1997) 125.
[27] M. Vallet-Regi, L.M. Rodriguez-Lorenzo, C.V. Ragel, A.J. Salinas, J.M. Gonzalez-Calbet, Control of structural type and particle size in alumina synthesized by the spray pyrolysis method, Solid State Ionics 101–103 (1997) 197.
[28] P. Fortunato, A. Reller, H.R. Oswald, Generation of mixed metal oxides by use of an ultrasonic aerosol thermal decomposition process, Solid State Ionics 101–103 (1997) 85.
[29] R.J. Lang, Ultrasonic atomization of liquids, J. Acoust. Soc. Am. 34 (1) (1962) 6.
[30] V. Jokanovic, D. Janackovic, D. Uskokovic, Influence of aerosol formation mechanism by an ultrasonic field on particle size distribution of ceramic powders, Ultrasonics Sonochem. 6 (1999) 157.
[31] D. Janackovic, V. Jokanovic, L. Kostic-gvozdenic, D. Uskokovic, Synthesis of mullite nanostructured spherical powder by ultrasonic spray pyrolysis, Nanostruct. Mater. 10 (3) (1998) 341.
[32] G.L. Messing, S.C. Zhang, G.V. Jayanthi, Ceramic powder synthesis by spray pyrolysis, J. Am. Ceram. Soc. 76 (1993) 2707.
[33] D. Bernache-Assolant, Une presentation des fondements de I'etude de la morphologie des poudres, des agregats et des frittes en insistant sur la caracterisation des surfaces et interfaces. Pour etudiants ingenieurs, chercheurs et industriels, Chimie, physique du frittage I Didier Bernache-Assollant. Hermes Science Publications, Paris, 1993, 350 pp. Illustration, 24 cm × 16 cm (FORCERAM). Bibliography, pp. 329–339. Index, pp. 345–348, ISBN 2-86601-343-3, 1993.
[34] F. Boulc'h, E. Djurado, Structural changes of rare-earth-doped, nanostructured zirconia solid solution, Solid State Ionics 157 (2003) 335.